Smart Mater. Struct. **18** (2009) 115025 (8pp) doi:10.1088/0964-1726/18/11/115025

Vibration energy harvesting using macro-fiber composites

Yaowen Yang[1,3], **Lihua Tang**[1] **and Hongyun Li**[2]

[1] School of Civil and Environmental Engineering, Nanyang Technological University, 50 Nanyang Avenue, 639798, Singapore
[2] Department of Engineering Mechanics, Shanghai Jiao Tong University, 1954 Huashan Road, Shanghai 200030, People's Republic of China

E-mail: cywyang@ntu.edu.sg, lihuatang@pmail.ntu.edu.sg and hyli@sjtu.edu.cn

Received 21 December 2008, in final form 26 June 2009
Published 15 September 2009
Online at stacks.iop.org/SMS/18/115025

Abstract
The decreasing energy consumption of today's portable electronics has invoked the possibility of energy harvesting from the ambient environment for self-power supply. One common and simple method for vibration energy harvesting is to utilize the direct piezoelectric effect. Compared to traditional piezoelectric materials such as lead zirconate titanate (PZT), macro-fiber composites (MFC) are characterized by their flexibility on large deformation. However, the energy generated by MFC is still far smaller than that required by electronics at present. In this paper, a vibration energy harvesting system prototype with MFC patches bonded to a cantilever beam is fabricated and tested. A finite element analysis (FEA) model is established to estimate the output voltage of the MFC harvester. The energy accumulation procedure in the capacitor is simulated by using the electronic design automation (EDA) software. The simulation results are validated by the experimental ones. Finally, to optimize the efficiency of energy harvesting, the effects of the electrical properties of MFC as well as the geometric configurations of the cantilever beam and MFC are parametrically studied by combining the FEA and EDA simulations.

(Some figures in this article are in colour only in the electronic version)

1. Introduction

With the advances in integrated circuitry, energy consumption of today's electronics continues decreasing, invoking the possibility for micro-electromechanical systems, wireless sensors and portable electronics to harvest energy from the ambient environment for self-power supply. There are many energy sources available in the environment but which are still not well utilized, such as the vibration energy. One simple method for vibration energy harvesting is to utilize the direct piezoelectric effect. Compared to the traditional piezoelectric materials such as lead zirconate titanate (PZT), the macro-fiber composites (MFC) [1] are characterized by their flexibility on large deformation, which enables them to harvest energy from ambient vibration sources with little brittle risk and long lifespan. However, the current and energy generated by MFC are still far from fulfilling the consumption requirements of most portable electronics at present.

In the past few years, many studies have been conducted on the energy generation ability of piezoelectric materials. Umeda *et al* [2] investigated the efficiency of a piezoelectric vibrator which converts the impact vibration energy into electrical energy. Ramsey and Clark [3] investigated the feasibility of using a piezoelectric transducer as a power supply for a bioMEMS application. Since polyvinylidene fluoride (PVDF) exhibits considerable flexibility compared to PZT, Kymissis *et al* [4] developed a parasitic power harvester in shoes to gather energy during walking using PVDF. As a new piezoelectric material, the energy harvesting capability of MFC has not been fully investigated. Sodano *et al* [5] compared the efficiencies of three piezoelectric materials, i.e. the traditional PZT, a quick pack actuator and MFC. It was concluded that MFC is less efficient compared to the conventional piezoelectric materials, but how to improve the efficiency of the energy harvesting of MFC was not mentioned. If the efficiency of MFC could be improved, it is expected to be more applicable than PZT in real applications because of its attractive property of flexibility.

[3] Author to whom any correspondence should be addressed.

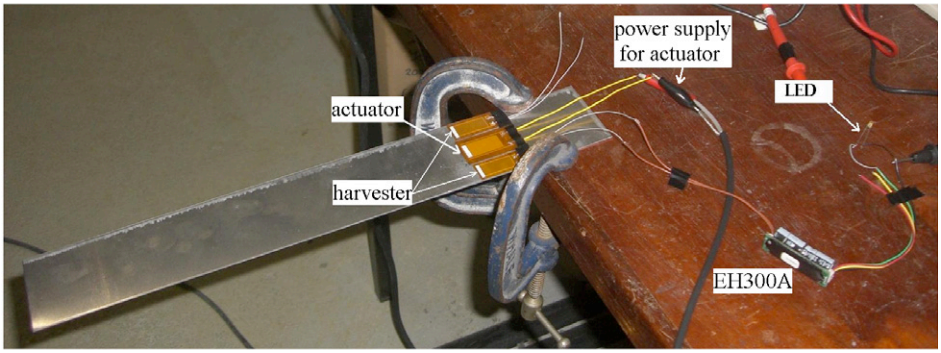

Figure 1. MFC energy harvesting system prototype.

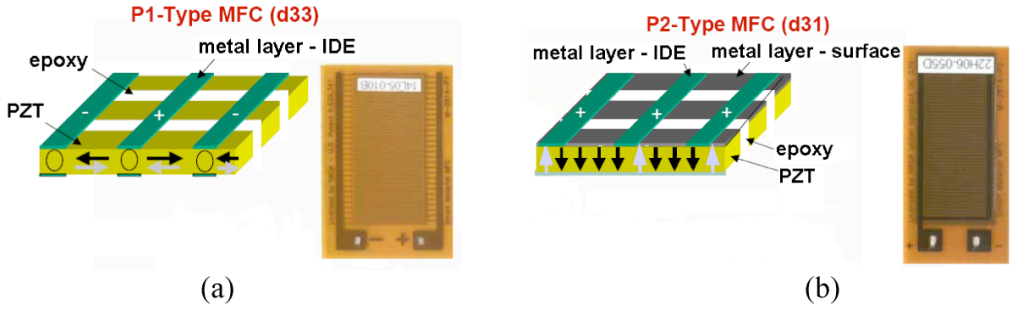

Figure 2. P1- and P2-type MFCs: (a) P1-type and (b) P2-type.

Improvement of the energy harvesting efficiency can be achieved in two ways. The first way is to improve the power output from the harvester. This can be achieved by changing the geometric configuration of the system or utilizing multiple pieces or a stacked configuration of piezoelectric materials [6, 7]. For a cantilever beam system, the length, width, thickness, beam shape and free end proof mass can be the candidate parameters to increase the vibration amplitude and to improve the strain-induced energy output. Jiang *et al* [8] modeled a cantilever bimorph with a proof mass attached to its free end and studied the effect of physical and geometrical parameters on the performance of power generation. Roundy *et al* [9] stated that, for the same volume of PZT, a trapezoidal cantilever could generate more than twice the energy as a rectangular beam.

The second way to improve the efficiency of energy harvesting is to enhance the power extraction ability using an optimized energy harvesting circuit. Many researchers have investigated different energy storage methods and attempted to develop an optimized circuit for energy extracting. Sodano *et al* [10] compared the efficiency of a capacitor and a nickel metal hydride battery as energy storage media. Ottman [11] developed an adaptive approach for energy harvesting from a mechanically excited piezoelectric element. By using a DC–DC converter with an adaptive control algorithm, the energy harvested was four times that of direct charging without the converter. Subsequently, a self-adaptive power harvesting circuit using the techniques termed 'synchronous electric charge extraction' [12] and 'synchronous switch harvesting on inductor' [13] has been developed and results showed that the synchronous circuit was able to increase power transfer by 400%. Yet, the additional electronics for monitoring and power management, on the other hand, consumed some of the energy harvested. A more efficient circuit is still under development.

In this paper, a vibration energy harvesting system prototype with MFC patches on a cantilever beam is developed. The output voltage of the MFC harvester is experimentally tested and estimated using the finite element method (FEM). Subsequently, the procedure of energy storing in the capacitor is simulated using the electronic design automation (EDA) software. The results are verified with the experimental ones. By combining the FEM and EDA simulations, parametric analysis is conducted to evaluate the effects of system parameters for optimal power harvesting.

2. Experimental study

The energy harvesting system is composed of an aluminum cantilever beam, one piece of P1-type MFC as actuator and two pieces of P2-type MFCs as harvesters, an energy harvesting circuit EH300A, a small LED bulb and a power supply to the actuator. The entire system is shown in figure 1. Note that the P1-type MFC actuator is used for a good controllable excitation of the system. It is not needed in the practical application.

The P1-type MFC utilizes the d_{33} piezoelectric effect (figure 2) to serve as the actuator to excite the beam. So the beam vibration amplitude can be tuned by altering the voltage input to the actuator. The two P2-type MFCs, which utilize the d_{31} effect (figure 2), are attached next to the P1-type MFC, serving as energy harvesters. The reasons for choosing a P1-type MFC as actuator are: (1) d_{33} is larger than d_{31};

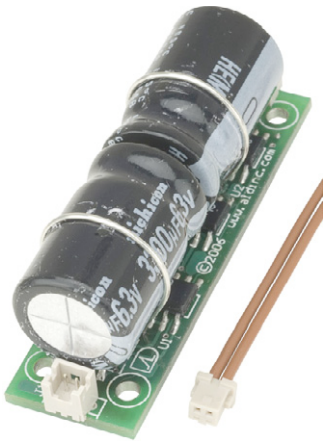

Figure 3. EH300A.

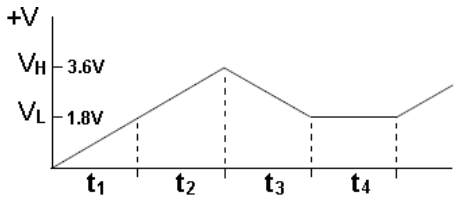

Figure 4. Voltage waveform across the capacitor bank in EH300A (from EH300A datasheet [15]).

(2) the operational voltage of the P1 type ranges from −500 to +1500 V [14], which enables it to be suitable for actuation, while the operational voltage of the P2 type is only −60 to +360 V and (3) the interdigital electrode configuration of the P1-type MFC limits the current output, which is not favorable for energy extraction. Two pieces of P2-type MFC harvesters are used to test the efficiency of the harvesting system for three cases, i.e. one single MFC, two MFCs electrically connected in series and then in parallel.

For the energy harvesting circuit, we utilize an EH300A module (figure 3), developed by Advanced Linear Devices, Inc [15]. When an energy source starts to inject energy into the inputs of the EH300A module in the form of electrical charge impulses, these charge packets are collected and accumulated in an internal storage capacitor bank. Figure 4 shows the waveform of the voltage across the capacitor bank in the EH300A. Initially, the voltage across the capacitor bank, $+V$, starts at 0.0 V. When $+V$ reaches V_H, the module output (V_P) is enabled to supply power to a load. In this study, the load is an LED bulb. As power is drawn by the LED from the capacitor bank during time duration t_3 (figure 4), $+V$ decreases. When it reaches V_L, the output V_P switches off and stops supplying any further power. The charging cycle will restart until V_H is reached again. During each charging cycle when $+V$ increases from V_L to V_H or energy is delivered to the load, around 30 mJ of energy (taken from the datasheet of EH300A [15]) is accumulated or released. In the experiment, time t_2 in figure 4 for different cases is our concern since it reflects the efficiency of energy harvesting of the system. The shorter it is, the higher is the efficiency.

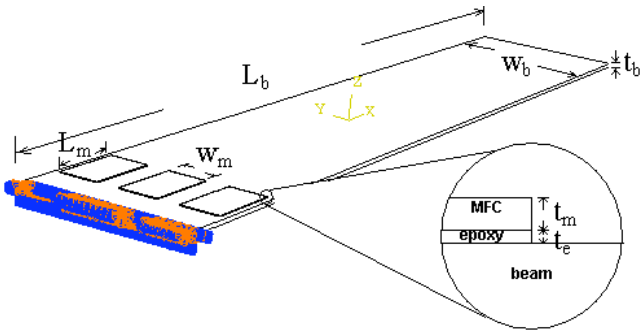

Figure 5. Geometric configuration of cantilever beam with MFC patches.

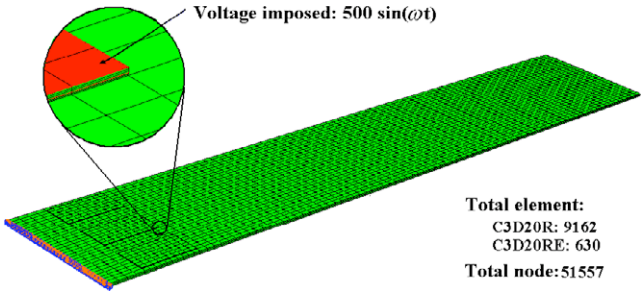

Figure 6. Finite element model.

Table 1. Material and geometric parameters of MFC and cantilever beam.

Item	Value
MFC active area dimensions (both P1- and P2-type)	28 mm × 14 mm × 0.25 mm
MFC piezoelectric constant d_{33}	3.74×10^{-10} C N^{-1}
MFC piezoelectric constant d_{31}	1.7×10^{-10} C N^{-1}
MFC dielectric constant	1.5×10^{-8} F m^{-1}
MFC elastic constants	$E_1 = 30.34$ GPa, $E_3 = 15.86$ GPa, $v_{13} = 0.31$, $G_{13} = 5.52$ GPa
MFC density	7500 kg m^{-3}
Epoxy dimensions	28 mm × 14 mm × 0.1mm
Epoxy elastic constants	$E = 0.1$ GPa, $v = 0.38$
Epoxy density	2200 kg m^{-3}
Aluminum beam dimensions	350 mm × 62 mm × 1.5 mm
Aluminum elastic constants	$E = 68$ GPa, $v = 0.35$
Aluminum density	2700 kg m^{-3}

3. Finite element modeling

To determine the ability of energy generation of the MFC, a finite element model is developed using the commercial code ABAQUS6.6 to calculate the voltage output from the MFC. The geometric configuration is shown in figure 5. The parameters of the energy harvesting system are listed in table 1. The mesh of the finite element model is shown in figure 6. The epoxy and aluminum beam are modeled using the reduced second-order solid element, i.e. C3D20R, and the MFC actuator and harvesters are modeled using the piezoelectric element, i.e. C3D20RE.

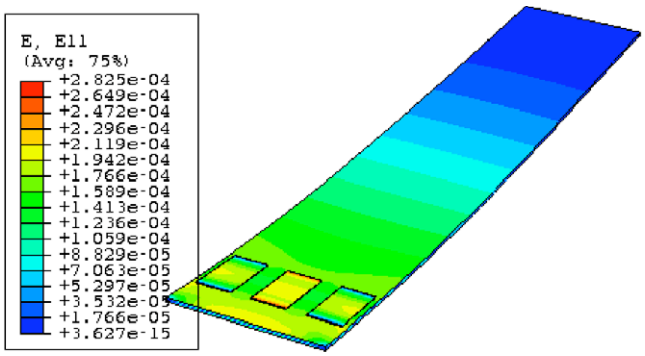

Figure 7. Strain and electrical potential distribution at the first natural frequency.

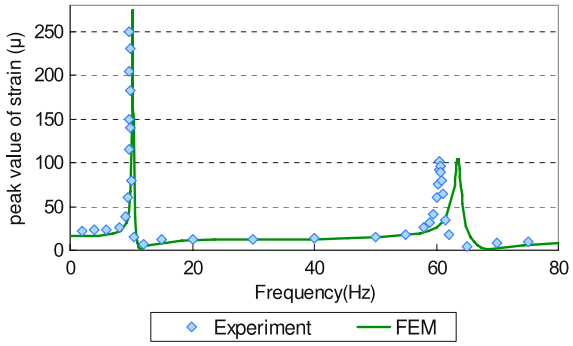

Figure 8. Peak value of strain at the center of the top surface of the MFC harvester.

3.1. Electrode modeling

The entire top and bottom surfaces of the P2-type MFC are covered by electrodes. In finite element analysis (FEA), the equation constraint [16] should be imposed on the electrical potential degrees of the surface nodes to ensure a uniform potential, which simulates the real electrodes. For the P1-type MFC actuator, it is quite difficult to directly model the interdigital electrodes. For convenience of analysis, the P1-type MFC will be equivalently converted to a P2-type MFC so that the top surface and bottom surface are modeled as electrodes, as shown in figure 6. The voltage load on the P1-type MFC actuator is applied by setting the potential on the bottom electrode to be zero and imposing the sinusoidal electrical potential on the top electrode. The equivalent conversion should ensure that the piezoelectric and electrical properties of the P1-type MFC remain unchanged. For the piezoelectric property, when applying the same voltage, the strain generated by the MFC should be the same:

$$d'_{31}\frac{V}{t_m} = d_{33}\frac{V}{e_m} \tag{1}$$

where $t_m = 0.25$ mm and $e_m = 0.5$ mm are the thickness and the distance between two neighboring interdigital electrodes of the P1-type MFC, respectively. Hence, the equivalent d'_{31} parameter applied in FEA is calculated as 1.87×10^{-10} C N^{-1}. Also, the dielectric constant 15×10^{-8} F m^{-1} before conversion should be changed to 0.3×10^{-8} F m^{-1} after conversion such that the capacitance is still 5 nF, as for the original P1-type MFC.

3.2. Rayleigh damping

In FEA, the damping effect should be considered, otherwise the calculation would be terminated because of the convergence problem near the beam resonance. Both the energy extracted from the MFC harvesters and the damping from the structural material contribute to the entire damping effect of the system. However, in FEA, only the open circuit voltage of the MFC harvester is calculated and no energy is removed from the system, in which case we assume that the damping of the system is only attributed to the damping of the beam material. Here, the Rayleigh damping [16] is considered for the aluminum beam:

$$\xi_i = \frac{1}{2}\left(\frac{\alpha}{\omega_i} + \omega_i\beta\right) \tag{2}$$

where α and β are the unknown parameters and ω_i is the frequency of the ith vibration mode. To obtain α and β, the damping ratios for the first and second resonance modes should be experimentally determined. Usually, the log decrement method [17] can be utilized to measure the damping ratio at the resonance frequency:

$$\xi = \frac{1}{2\pi n}\ln\frac{A_1}{A_{n+1}} \tag{3}$$

where A_1 and A_{n+1} are the first and the $(n+1)$th peak value of voltage recorded by a digital multimeter. A simple experiment has been conducted to record the free vibration response of the system. Using the experiment data and equation (3), the damping ratios for the first and second modes are obtained as $\xi_1 = 0.0064$ and $\xi_2 = 0.0077$. Applying ξ_1 and ξ_2 to equation (2), the two parameters of the Rayleigh damping can be determined as $\alpha = 0.66$ and $\beta = 3.544 \times 10^{-5}$.

3.3. Results of steady-state analysis

Figure 7 shows the strain distribution of the cantilever beam and MFC harvesters at the first natural frequency. Figures 8 and 9 show the peak value of strain and RMS voltage output from one single MFC harvester, respectively. It is noted that the values of strain and voltage from the FEA match well with the experimental results except for minor shifts on the frequency axis. This could be attributed to the fact that the cantilever beam is not perfectly clamped, as shown in figure 1. For the first mode, the natural frequencies obtained from the experiment and simulation results are 9.75 Hz and 10.269 Hz, respectively, and the RMS voltage outputs are 11.5 V and 10.8 V, respectively. The differences between the experiment and simulation results are around 5%. Therefore, the finite element model is able to accurately evaluate the voltage output of the MFC harvester.

In energy harvesting applications with ultra-low frequency (around 1 Hz) impulse input, the cantilever beam will

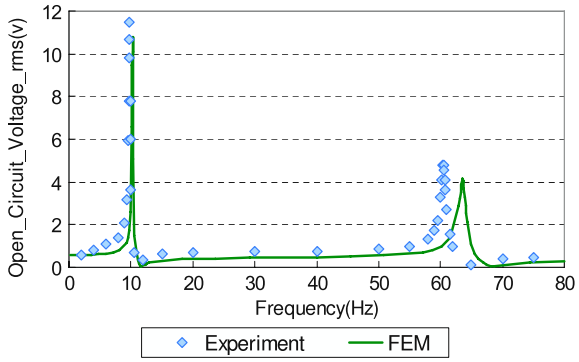

Figure 9. RMS voltage output of the MFC harvester.

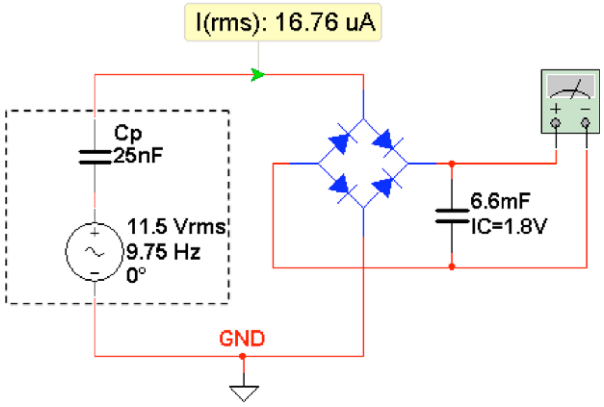

Figure 10. Circuit of the energy harvesting system.

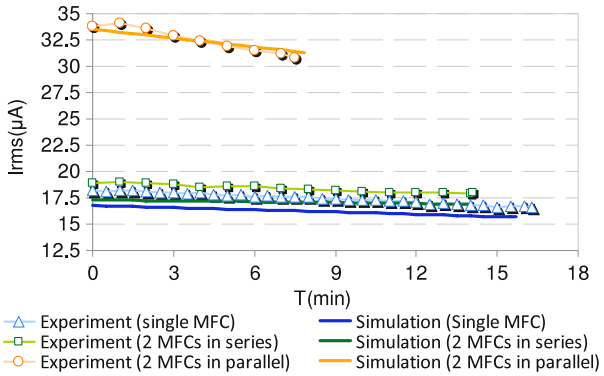

Figure 11. Charging curves for three cases at the first natural frequency.

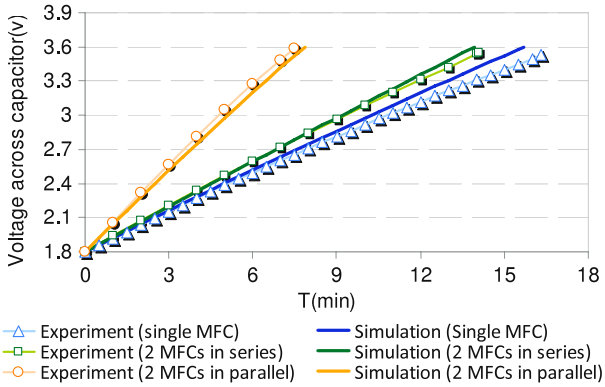

Figure 12. Energy storing procedure for three cases at the first natural frequency.

experience free vibration with damping at the first natural frequency. At this resonance frequency, the MFC harvester will be subjected to the maximum strain and hence release the maximum output voltage, as shown in figure 9. As a result, the efficiency of energy harvesting at resonance is of great importance. In later sections, the efficiencies of MFC harvesters are considered at the first natural frequency.

4. Electronic simulation

The voltage output of the MFC harvester can be obtained from FEA. However, based on these results, we still cannot evaluate the power available to be extracted from the MFC harvester. Actually, because of the intrinsic capacitance, the power generated by the MFC harvester will be recovered back to the source. As a result, the efficiency of the energy harvesting system depends on the amount of energy extracted and stored from the MFC. The EDA software Multisim10.0 by National Instrument is utilized to simulate the energy extraction and storing procedures from the MFC harvester. Figure 10 shows the circuit of the energy harvesting system. The EH300A module is simplified as a full-wave rectifier and a capacitor bank, and the power management module in EH300A is neglected. As the first natural frequency of the cantilever beam is around 10 Hz, the impedance from the internal capacitance (measured as 25 nF in the experiment) is quite large, around 637 kΩ. The equivalent circuit [18] of the MFC harvester is composed of a voltage source in series with its internal capacitance, as shown in the dashed box in figure 10, which is similar to that for the conventional piezoelectric material.

4.1. Efficiency at first natural frequency

The efficiency of the energy harvesting system at the first natural frequency is tested for three cases, namely, one single MFC, two MFCs electrically connected in series and then in parallel. Figures 11 and 12 illustrate the history of charging current to the EH300A and the energy storing procedure in the capacitor bank of the EH300A, respectively. Again, the simulation results match well with the experimental ones.

Table 2 lists the time t_2 (refer to figure 4) for 30 mJ accumulated in the EH300A and the average power of energy storing from the experiment and electronic simulation for the three cases at the first natural frequency. It is noted that MFCs electrically connected in parallel generate the largest charging current to the EH300A and hence are the most efficient to charge the energy storage capacitor with a capacitance of 6.6 mF in the EH300A.

Table 2. Energy harvesting performance for three cases.

MFC connection	Capacitance (nF)	Open circuit Vrms (V)	Experiment t_2 (s)	Experiment Average power (μW)	Simulation t_2 (s)	Simulation Average power (μW)
Single	25	11.5	978	30.67	942	31.85
In series	12.5	21.5	845	35.50	835	35.93
In parallel	50	11.85	450	66.67	471	63.69

Table 3. Energy harvesting performance of MFC with various dielectric constants.

MFC dielectric constant (F/m)	Open circuit Vrms (V)	Capacitance (nF)	Time for 30 mJ accumulated (s)	Average power (μW)
1.00×10^{-8}	15.946 6	16.667	860.403	34.87
1.25×10^{-8}	12.866 6	20.833	889.418	33.73
1.5×10^{-8}(*)	10.796 7	25	922.260	32.53
1.75×10^{-8}	9.299 7	29.17	960.776	31.22
2.00×10^{-8}	8.166 94	33.33	1004.428	29.87

Table 4. Energy harvesting performance of MFC with various thicknesses.

MFC thickness (mm)	First natural frequency (Hz)	Open circuit Vrms (V)	Capacitance (nF)	Time for 30 mJ accumulated (s)	Average power (μW)
0.1	10.205	5.41591	62.5	1028.865	29.16
0.15	10.227	7.49473	41.67	912.697	32.87
0.2	10.249	9.24628	31.25	905.464	33.13
0.25(*)	10.269	10.7967	25	922.260	32.53
0.3	10.291	12.1485	20.833	952.331	31.50
0.35	10.311	13.3117	17.857	991.425	30.26

Table 5. Energy harvesting performance of MFC multilayer stack configurations.

Multilayer number	First natural frequency (Hz)	Open circuit Vrms (V)	RMS tip deflection (mm)	Capacitance (nF)	Time for 30 mJ accumulated (s)	Average power (μW)
1(*)	10.269	10.796 7	9.28	25	922.260	32.53
2	10.367	7.629 01	8.64	50	732.332	40.97
3	10.436	5.477 82	8.18	75	823.795	36.42
4	10.487	4.078 01	7.84	100	1142.759	26.25

5. Optimization of energy harvesting system

As shown above, the FEA and EDA simulations are able to accurately evaluate the voltage output of MFC harvesters and the energy storage in the EH300A. By combing the two simulations, a parametric analysis can be performed to estimate the optimal power generation of the system. In table 2 it is noted that the parallel and series connections alter both the capacitance and the MFC output voltage. The parallel connection doubles the capacitance of the harvesting system without changing the voltage output, while the series connection halves the capacitance but doubles the MFC voltage output. The results of increased average power for energy storage to the EH300A indicate that both the capacitance of MFC harvesters and the voltage output are the key factors to optimize the efficiency of the energy harvesting system.

5.1. Effect of MFC capacitance

The capacitance of the MFC can be changed by the dielectric constant, the thickness and the area of the MFC.

5.1.1. Dielectric constant. With the advances in material science, the dielectric constant of piezoceramics can be changed during fabrication. Here, five values of dielectric constant are considered to study its effect on the performance of the energy harvesting system. In contrast to expectations, the dielectric constant fails to show significant influence on the energy harvesting power, as demonstrated in table 3 This should be attributed to the accompanying variation of output voltage from the MFC harvester. In tables 3–5, the values with '*' are the actual values of the MFC harvester in the experiment.

5.1.2. Thickness of MFC. With a decrease in MFC thickness, the capacitance will relatively increase. To our disappointment, varying the MFC thickness also fails to improve the power extraction from the MFC, as shown in table 4.

5.1.3. MFC stack configuration. The fact that changing the dielectric constant or MFC thickness cannot improve the energy harvesting power is probably attributed to that the

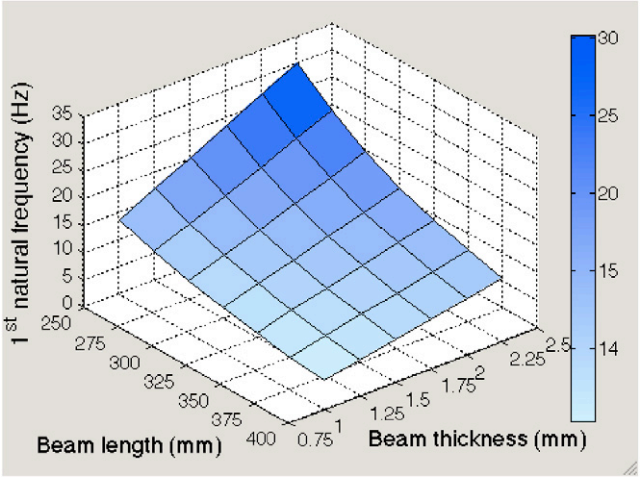

Figure 13. First natural frequency with various beam dimensions.

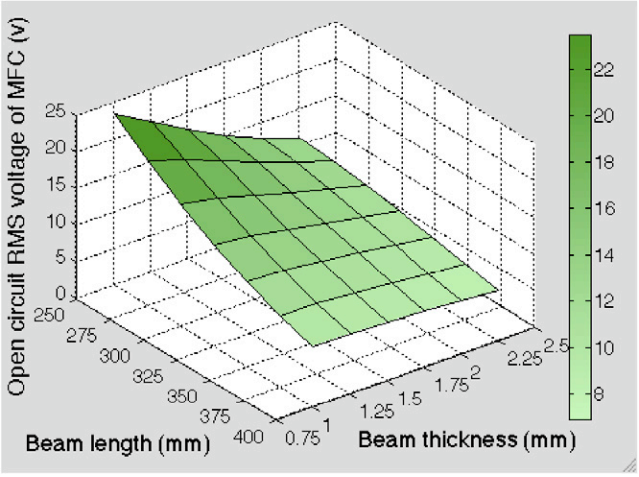

Figure 14. MFC voltage output with various beam dimensions.

charges available to be extracted do not increase or even decrease for the specific MFC area. As for increasing the area of the MFC, multiple MFCs electrically connected in parallel have been proven the most efficient. But increasing the MFC area as in the experiment is not suitable for a wearable energy harvesting application. Thus, we try another way to equivalently increase the area of the MFC, i.e. using the MFC stack configuration where multiple MFCs are geometrically connected in series while electrically in parallel, which is favorable for reducing the size of the energy harvesting system. In table 5, it is observed that for the two-layer MFC stack configuration, the energy extraction power can achieve a maximum increase of 26% compared to the non-stack configuration. But for more layers of MFCs, the energy extraction power decreases. This is due to the fact that the multilayer stack configuration limits the flexibility of the MFC, which in turn reduces the beam vibration and hence the output voltage, as shown in table 5.

5.2. Varying beam dimensions

The above results on the variation of MFC capacitance affirm that the MFC voltage output is another important factor that affects the system performance. In this section, the beam dimensions will be optimized to increase the beam vibration amplitude. Besides, the beam dimensions will also affect the first natural frequency. Here, only the thickness and length of the beam are considered for optimization. With larger thickness and smaller length, a higher natural frequency is expected, while with larger thickness and length, lower voltage output from the MFC harvester is expected, as shown in figures 13 and 14.

With the given impedance, higher open circuit voltage means higher current, which is favorable for charge accumulation in a capacitor or battery. However, besides the capacitance in the capacitive energy harvesting circuit (figure 10), the impedance also depends on the excitation frequency. In this work, we only consider the power achieved at the first natural frequency. The structural configuration for maximum open circuit voltage does not ensure the maximum

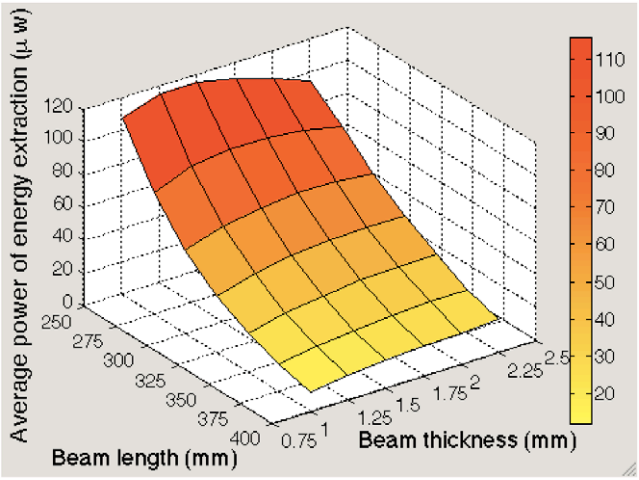

Figure 15. Average power of energy extraction with various beam dimensions.

power output at the first natural frequency (used as the excitation frequency). The maximum power output is achieved with the trade-off between the open circuit voltage and the natural frequency, as shown in figures 13–15. With seven values of length and six values of thickness in the simulation, the optimized power can be obtained at length = 250 mm and thickness = 1.5 mm, as shown in figure 15.

5.3. Optimized energy harvesting performance

Based on the above parametric analysis, for optimal energy harvesting performance, it is recommended to use the two-layer MFC stack configuration with the beam dimensions of 250 mm × 62 mm × 1.5 mm. The energy harvesting power can be optimized as 151.6 μW when the beam vibrates at the first natural frequency, as listed in table 6.

6. Conclusion

In this paper, an energy harvesting system prototype with MFC patches on a cantilever beam is developed and the efficiency

Table 6. Optimized performance of the MFC energy harvesting system.

First natural frequency (Hz)	Open circuit Vrms (V)	Capacitance (nF)	Time for 30 mJ accumulated (s)	Average power (μW)
20.575	12.702	50	197.94	151.6

of energy harvesting is tested. A finite element model for the system is developed and verified with the experimental results, showing its capability for accurate evaluation of the voltage output from the MFC harvesters. Subsequently, the procedure of energy extraction and storing to the capacitor in the EH300A is simulated by using the electronic design automation (EDA) software. By combining the FEM and EDA simulations, parametric analysis is conducted to optimize the energy harvesting performance of the system. It is found that, with the MFC stack configuration with two layers and the beam dimensions of 250 mm $\times$ 62 mm $\times$ 1.5 mm, energy extraction from the MFC harvesters can be optimized. The optimized power of 151.6 μW is achieved when the beam vibrates at the first natural frequency. It is demonstrated that the combined FEM and EDA simulations are useful tools for evaluating and optimizing the efficiency of MFC-based energy harvesting systems, which are also applicable to other piezoelectric material-based systems.

References

[1] Werlink R J, Bryant R G and Manos D 2002 Macro fiber piezocomposite actuator poling study *NASA/TM-2002-211434*

[2] Umeda M, Nakamura K and Ueha S 1996 Analysis of transformation of mechanical impact energy to electrical energy using a piezoelectric vibrator *Japan. J. Appl. Phys.* **35** 3267–73

[3] Ramsey M J and Clark W W 2001 Piezoelectric energy harvesting for bio MEMS applications *Proc. SPIE* **4332** 429–38

[4] Kymissis J, Kendall D, Paradiso J and Gershenfeld N 1998 Parasitic power harvesting in shoes *2nd IEEE Int. Conf. on Wearable Computing* pp 132–9

[5] Sodano H A, Inman D J and Park G 2005 Comparison of piezoelectric energy harvesting devices for recharging batteries, *J. Intell. Mater. Syst. Struct.* **16** 799–807

[6] Ng T H and Liao W H 2005 Sensitivity analysis and energy harvesting for a self-powered piezoelectric sensor *J. Intell. Mater. Syst. Struct.* **16** 785–97

[7] Platt S R, Farritor S and Harder H 2005 On low-frequency electric power generation with PZT ceramics *IEEE/ASME Trans. Mechatronics* **10** 240–52

[8] Jiang S, Li X, Guo S, Hu Y, Yang J and Jiang Q 2005 Performance of a piezoelectric bimorph for scavenging vibration energy *Smart Mater. Struct.* **14** 769–74

[9] Roundy S, Leland E S, Baker J, Carleton E, Reilly E, Lai E, Otis B, Rabaey J M, Wright P K and Sundararajan V 2005 Improving power output for vibration-based energy scavengers *IEEE Pervasive Comput.* **4** 28–36

[10] Sodano H A, Inman D J and Park G 2005 Generation and storage of electricity from power harvesting devices *J. Intell. Mater. Syst. Struct.* **16** 67–75

[11] Ottman G K 2002 Adaptive piezoelectric energy harvesting circuit for wireless remote power supply *IEEE Trans. Power Electron.* **17** 669–76

[12] Lefeuvre E, Badel A, Richard C and Guyomar D 2005 Piezoelectric energy harvesting device optimization by synchronous electric charge extraction *J. Intell. Mater. Syst. Struct.* **16** 865–76

[13] Badel A, Guyomar D, Lefeuvre E and Richard C 2005 Efficiency enhancement of a piezoelectric energy harvesting device in pulsed operation by synchronous charge inversion *J. Intell. Mater. Syst. Struct.* **16** 889–901

[14] http://www.smart-material.com/MFC/MFC_specs.php

[15] EH300A datasheet http://www.aldinc.com/pdf/EH300ds.pdf

[16] 2006 *ABAQUS Analysis User's Manual* Version 6.6-1, Section 28.2.1: linear constraint equations, and section 20.1.1: Material damping

[17] Meirovitch L 2005 *Fundamentals of Vibrations* (New York: McGraw-Hill)

[18] Park C H 2001 On the circuit model of piezoceramics *J. Intell. Mater. Syst. Struct.* **12** 515–22